Ariel Federico (Orcid ID: 0000-0001-8478-8808)
LUCERO LEANDRO (Orcid ID: 0000-0003-4453-8964)

Differential chromatin binding preference is the result of the neo-functionalization of the TB1 clade of TCP transcription factors in grasses

Natanael Mansilla[1], Camille Fonouni-Farde[1], Federico Ariel[1] and Leandro Lucero[1,*]

[1] Instituto de Agrobiotecnología del Litoral, CONICET, FBCB/FHUC, Universidad Nacional del Litoral, Colectora Ruta Nacional 168 km 0, 3000, Santa Fe, Argentina

[*] Correspondence to be sent to:
Leandro Lucero
Email: lucero@santafe-conicet.gov.ar

Received: *28 September 2022*
Accepted: *29 November 2022*

Key words: Chromatin Binding Preference; Gene Neo-functionalization; Grasses; TB1; TCP Transcription Factors; *Zea mays*.

ORCID
Mansilla Natanael 0000-0001-6052-3223
Fonouni-Farde Camille 0000-0001-5423-8434
Ariel Federico 0000-0001-8478-8808
Lucero Leandro 0000-0003-4453-8964

Summary

- The understanding about neo-functionalization of plant transcription factors (TFs) after gene duplication has been extensively focused on changes in protein-protein interactions, the expression pattern of TFs, or the variation of *cis*-elements bound by TFs. Yet, the main molecular role of a TF, *i.e*. its specific chromatin binding for the direct regulation of target gene expression, continues to be mostly overlooked.
- Here, we studied the TB1 clade of the TEOSINTE BRANCHED 1, CYCLOIDEA, PROLIFERATING CELL FACTORS (TCP) TF family within the grasses (Poaceae).
- We identified an Asp/Gly amino acid replacement within the TCP domain, originated within a paralog TIG1 clade exclusive for grasses. The heterologous expression of *Zea mays* TB1 and its two paralogs BAD1 and TIG1 in Arabidopsis mutant plants lacking the TB1 ortholog BRC1 revealed distinct functions in plant development. Notably, the Gly acquired in the TIG1 clade does not impair TF homodimerization and heterodimerization, while it modulates chromatin binding preferences. We found that *in vivo* TF recognition of target promoters depends on this Asp/Gly mutation and directly impacts downstream gene expression and subsequent plant development.
- These results provided new insights into how natural selection fine-tunes gene expression regulation after duplication of TFs to define plant architecture.

Introduction

Transcription factors (TFs) are key players in the modulation of gene expression, which, in turn, is a driving force for the evolution of developmental innovations. In the plant kingdom, TFs are particularly subjected to pervasive duplications, paving the way for the evolution of gene expression regulation and subsequent phenotypic variation (Hughes et al. 2014; Lai et al. 2020). Adaptive selection is considered a major driving force of molecular evolution after gene duplication through the neo-functionalization of paralog genes (Ohno 1970). In this sense, it is expected that positively selected or adaptive sites fixed after gene duplication impact on the protein activity producing molecular innovations. So far, studies addressing the impact of TFs in the evolution of innovations in plants have been mostly focused on the changes in protein-protein interactions (Bartlett et al. 2016a), the expression pattern of TF encoding genes (Lin and Rausher 2021a; Lin and Rausher 2021b), or the presence of mutations downstream the *cis*-elements recognized by TFs in a DNA sequence (Borba et al. 2018; de Meaux 2018; Wang et al. 2021). Studies analyzing the mechanistic of TF activity across plant evolution remain scarce (Wang et al. 2015; Bartlett et al. 2016a; Lai et al. 2020; Lyu et al. 2020). Considering that the chromatin binding activity of TFs is essential for the direct activation or repression of gene expression, a key question that remains to be answered is how TF evolution at the protein level affects their binding activity. This crucial molecular function of TFs thus emerges as a key facet to characterize them from an evolutionary perspective.

The TCP family of TFs is unique to plants and its members are found since the Charophyta algae (Navaud et al. 2007). The distinctive feature of these TFs is the shared presence of a DNA binding domain denominated TCP (Cubas et al. 1999). The TCP family was named after the discovery of the three founding members, TEOSINTE BRANCHED1 (TB1) in maize (Doebley et al. 1995), CYCLOIDEA (CYC) in *Antirrhinum majus* L. (Luo et al. 1996), and PROLIFERATING CELL FACTORS (PCFs) in rice (Kosugi and Ohashi 1997). The biological roles of TCP TFs are highly diverse. They are involved in almost every aspect of plant development since terrestrialization (Busch et al. 2019; for reviews see: Uberti Manassero et al. 2013; Nicolas and Cubas 2016). The TCP family can be divided into two main classes, namely class I (PCF) and II TCP, further divided into two additional clades, namely CINCINNATA (CIN) and CYC/TB1 (Cubas et al. 1999). Studies performed in *Arabidopsis thaliana* L., indicated that the two classes of TCP TFs bind similar but distinct DNA elements. The class I TCP recognizes the GTGGGNCC motif while the class II prefers the GTGGNCCC *cis*-element (Kosugi and Ohashi 2002; Aggarwal et al. 2010). The first global binding preference analysis of TCP TFs revealed that the maize TCP TB1 recognized the consensus sequence of class II TCPs (Dong et al. 2019). More recently, it was

shown that the *Marchantia polymorpha* L. TCP1 also recognized the consensus sequence of the TCP family (Karaaslan et al. 2020), further supporting that sequence specificity is highly conserved among TCP TFs since plant terrestrialization. Therefore, how TCP TFs acquired or changed their preference to bind different sets of target genes is still an open question, especially intriguing for paralogs TFs.

In Poaceae (commonly referred to as grasses), one of the most studied TCP members is precisely TB1, given its pivotal role in maize domestication from the teosinte ancestor (Doebley et al. 1995). In maize, TB1 is responsible for the repression of axillary branch development through the control of apical dominance, defining the final plant architecture (Doebley et al. 1995). Interestingly, TB1 function is conserved between dicots and monocots (Aguilar-Martínez et al. 2007; Lewis et al. 2008; Igartua et al. 2020). *BRANCHED 1* (*BRC1*) was identified as the ortholog of *TB1* in the dicot *A. thaliana*, and its knockout results in an increased number of axillary branches (Aguilar-Martínez et al. 2007). The link between crop domestication and *TB1*-like genes was established in other species of the grass family, for instance with *OsTB1/FINE CULM1* (*FC1*) in rice (Takeda et al. 2003; Minakuchi et al. 2010), *INTERMEDIUM-C* (*INT-C*) in barley (Ramsay et al. 2011) and *TaTB1* in wheat (Dixon et al. 2018). Other grass *TB1*-like genes were characterized as key regulators of plant architecture, like *BRANCH ANGLE DEFECTIVE 1* (*BAD1*) in maize (Bai et al. 2012), *RETARDED PALEA1* (*REP1/OsTB2*) (Yuan et al. 2009; Lyu et al. 2020) and *TILLER INCLINED GROWTH* 1 (*TIG1*) (Zhang et al. 2019) in rice, or again *COMPOSITUM 1* (*COM1*) in barley (Poursarebani et al. 2020). Gene duplication is a hallmark of the TCP family, being also an important driving force for *TB1*-like gene diversification (Igartua et al. 2020). This highlights the need for a comprehensive phylogenetic framework to understand the evolution of TCP TFs in Poaceae, especially for the TB1 clade given its crucial role in crop evolution and domestication.

One of the major driving forces for gene neo-functionalization after duplication events is the fixation of adaptive residues (Ohno 1970; Conant and Wolfe 2008). There is a vast literature showing the incidence of positive selection in plant TFs (Viola et al. 2012; Wu et al. 2014; Bartlett et al. 2016a; Derbyshire et al. 2021; Zhang et al. 2021), even including *TB1*-like genes from the TCP family (Gübitz et al. 2003; Martín-Trillo et al. 2011). However, the implication of adaptive evolution in the binding preference of TFs to chromatin remains largely unknown. Here, we identified within the TB1-like clade, an Asp to Gly radical replacement in the TCP DNA binding-domain, after gene duplication exclusive to the *TIG1* subclade in the grass family. By combining phylogenetic, biochemical and functional analyses, we showed the incidence of this residue on chromatin binding and target gene expression regulation. Our results indicate that this adaptive site within the TCP domain might have facilitated the path to neo-functionalization in the TB1-like

clade through the modulation of the interaction with chromatin. Hence, our work provides novel insights into how natural selection can fine-tune the binding preference of paralog TFs to their target loci despite sequence identity, likely hinting at other features of the chromatin under selection.

Materials and Methods

Phylogenetic Analyses and Selection Test

TCP gene sequences were searched through BLAST using *Zea mays* L. *TB1* and *BAD1* as a query. The coding sequences (CDS) of all *TCP* genes from nine grass species and four outgroup species were retrieved from Phytozome 13 (Table S1). The 303 CDS sequences were translated into protein and then aligned with Muscle (Edgar 2004) as implemented in MEGA-X (Kumar et al. 2018). Model selection was achieved using ModelFinder (Kalyaanamoorthy et al. 2017), being the model TVM+F+R4 that best fits our data, according to the Bayesian Information Criterion. The Maximum likelihood (ML) tree was obtained using IQTREE2 (Nguyen et al. 2015), with 1000 ultrafast bootstrap replicates to estimate branch support. The phylogeny was drawn with Figtree (http://tree.bio.ed.ac.uk/software/figtree/).

To infer site-specific selective strengths operating on the TCP domain, an additional tree was generated using only *TB1*-like genes (previously identified in **Fig. 1a**), but including three additional out-group Monocot species (Table S1), aiming at further validating the tree topology and enhancing the detective power of the selection test. The in-paralog sequences of *Z. mays* within the TIG1 clade were pruned from the tree, retaining only the most similar sequence to OsTIG1, GRMZM2G060319 (used for later functional and molecular experiments). In addition, the two TIG1 sequences of wheat have a partial deletion of the TCP domain (**Fig. S2**, see later). We excluded them from the final tree used for the selection test to avoid any gap in the alignment of the TCP domain. Codon-base alignment were produced with webprank (http://www.ebi.ac.uk/goldman-srv/webprank/), in order to diminish the incidence of false positives in the discovery of adaptive residues. ML searches were conducted with IQTREE2, evaluating branch support with 1000 bootstrap replicates. Selection test was conducted using PAML v4.9 package (http://abacus.gene.ucl.ac.uk/software/paml.html) (Yang, 2007). The models M7 and M8a were used as implemented in CODEML. With these models, the non-synonymous/synonymous rate ratio omega = dN/dS was inferred, with omega = 1, omega < 1, and omega > 1 indicating neutral, negative, and positive selection, respectively. To determine if the alternative model (M8a) fits better than the null model (M7) (indicating positive selection), we

used a x^2 test using the likelihood ratio of both models. To inform the sites under positive selection we used the Bayes Empirical Bayes approach.

Cloning and Quickchange mutagenesis

Entry clones containing the complete CDS sequence of *Z. mays TB1* (UT5978), *BAD1* (UT1680) and *TIG1* (UT3439) in the pENTR-TOPO-D vector were obtained from Grassius (https://www.grassius.org/), and recombined in the destination vector pFAST-R05 (Shimada et al. 2010) or pAUL01 (Lyska et al. 2009) by LR reaction (following the manufacturer procedure (Thermofisher)) to add a GFP or HA tag at the 3' position. To introduce the G23D mutation in ZmTIG1 and the D23G mutation in ZmTB1, we performed *in vitro* mutagenesiswith Phusion enzyme (Thermo-Fisher Scientific), using the UT3439 and UT5978 entry clones as template. To introduce the stop codon for 5´ tagging in pFK241, *ZmTIG1* and *ZmTIG1-G23D* were sub-cloned in pENTR-3C using *BamH*I and *EcoR*I restriction enzymes. To sub-clone *ZmTIG1* and *ZmTIG1-G23D* in pAS054 and pAS059 vectors the same restriction enzymes were used removing the stop codon from the reverse primer. To sub-clone *ZmTB1* and *Zm*BAD1 in pAS054 and pAS059 vectors, we used *Kpn*I and *EcoR*I or *Sal*I and *Not*I restriction enzymes, respectively. These entry clones were then used for LR recombination. All the clones obtained here (**Table S2**) were confirmed by Sanger sequencing (Macrogen). The primers used are listed in the **Table S3**.

Plant material and transformation

Stable transformation of *A. thaliana* was performed by the floral dip method (Clough and Bent 2008). The *brc1-2* mutant in Columbia ecotype (col-0) used was described elsewhere. Transgenic lines were selected on half strength Murashige and Skoog (MS) plates supplemented with kanamycin. For transitory transformation of maize and rice, we used *Z. mays* B73 and *Oryza sativa* L. Kitaake seeds, respectively. Arabidopsis and *Nicotiana benthamiana* Domin plants were grown at 23°C in pots. Maize plants were grown in pots at 28°C in a CONVIRON-ADAPTIS-A1000 growing chamber. Rice seeds were germinated and grown on half strength MS medium. All the species used were grown in long-day photoperiod (16 h of light/8 h of dark). Light intensity used was 150 µmol m-2 s-1 for all the species, and 400 µmol m-2 s-1 for maize.

For agrobacterium-mediated transformations in *Z. mays* and *N. benthamiana* we used a slightly modified version of Zhang et al. (2020) protocol, using the GV3101 Agrobacterium strain. Briefly, 100 µL of saturated culture was inoculated on YEB-induced medium plates and the agrobacteria were grown at 28°C for 36 h. The cells were scraped and resuspended in 5 mL of washing solution

(10 mM $MgCl_2$, 100 µM acetosyringone). The agrobacteria were then diluted to an OD_{600} of 0.5 in an infiltration solution (¼MS [pH = 6.0], 1% sucrose, 100 µM acetosyringone, 50 µL/L Silwet L-77). For BiFC, the different combination were made using the ratio 2:2:1 (Interactor1: Interactor2:p19). For the IP assay, p19 was omitted to avoid problems with the HA tag. Plants were infiltrated using a 1 mL plastic syringe, kept in the light to dry the leaves for 1 h, and then kept in the dark for 16-24 h at room temperature. The transformed plants were then transferred back to the greenhouse for another 2–3 days before sample collection/microscopy analyses.
Rice protoplast isolation and transformation was achieved according to He et al. (2016), using 10 days-old plants. 20 µg of the pFK241 vector carrying ZmTIG1 or ZmTIG1-G23D were used for transformation.

Expression analyses

Total RNA was extracted with Trizol reagent. For Arabidopsis, we used 10-days-old pulled plants. For transient expression in maize and rice, samples were harvested three and one day after transformation, respectively. cDNA synthesis was performed using the High-Capacity cDNA Reverse Transcription Kit (Thermo-Fisher Scientific). The iTaq Universal SYBR Green supermix (BioRad) was used for amplicon detection in an Applied Biosystems StepOnePlus apparatus (Thermo-Fisher Scientific). Specific primers designed for RT-qPCR are listed in **Table S3**.

Chromatin Immunoprecipitation

ChIP experiments were performed as in Moison et al. (2021), using the ab290 and the ab6702 (Abcam) antibodies against GFP and IgG, respectively. Ten days-old whole plantlets were used for *A. thaliana* experiments. For *Z. mays*, the cotyledon and the first leaf of 10 days-old transiently transformed plants were used. The pFAST-R05 vector was used for GFP tagging in Arabidopsis and maize experiments. The samples of maize leaves were cross-linked three days after being transiently transformed. For the ChIP experiment in rice protoplasts, equal concentrations of isolated protoplasts (5×10^5) were transformed with the pFK241 vector carrying *ZmTIG1* or *ZmTIG1-G23D* CDS. Rice samples were harvested 24 h after transformation and cross-linked according to Lee et al. (2017). After harvesting the protoplasts, we continued as routinary. Primers used for RT-qPCR analyses are listed in **Table S3**.

Confocal laser scanning and Fluorescence microscopy (CLSM)

For CLSM, leaves infiltrated with the different constructs were imaged with a Leica TCS SP8 confocal laser scanning microscope. In the BiFC assay, samples were excited at 514 nm and detection was set at 520–560 nm for mCitrine. Laser intensity and photomultiplier detector gain were equal for all the samples. GFP samples were excited at 488 nm and the detection was set at 493–530 nm. In both cases, the chlorophyll fluorescence was collected at 640–670 nm and the transmitted light was also imaged. All the images were captured using a 10x or 20× lens. Image processing and quantification was carried out using Fiji software (Schindelin et al. 2012). For BiFC, at least ten different images for each combination of constructs were analyzed, quantifying the average nuclear mCitrine fluorescence intensity. Data were analyzed by the nonparametric Dunn's multiple comparisons test to evaluate significant differences. The Eclipse E200 Leica microscope was used to verify rice protoplast transformation.

Fluorometric measurements

GFP signal was quantified in at least six leaf discs. Samples were exited at 485nm and fluorescence was collected at 538nm using the fluorometer Fluoroskan Ascent FL (Thermo Fisher Scientific). Untransformed maize (from transient transformation assays) or *A. thaliana* (from *brc1-2* complemented plant lines) leaf discs were used to set the autofluorescence background.

Protein interaction assays

For protein interaction experiments we used *N. benthamiana* co-transformed leaves as described above. Samples and images were taken 72-hours after agrobacterium transformation. For BiFC assay, *ZmTIG1* or *ZmTIG1-G23D* were subcloned in the pAS054 and pA0S59 for N-mCitrine and C-mCitrine tagging. HaH11 clone was obtained from a previous report (Miguel et al. 2020). CLSM was used for image acquisition as described above.

The CoIP assay was performed with the ZmTIG1-HA (pAUL01 vector) and ZmTIG1-GFP or ZmTIG1-G23-GFP (pFAST-R05 vector) constructs. For Western blot analyses, proteins were separated by SDS-PAGE and transferred to Hybond-P (GE Healthcare) using standard protocols. Blots were probed with monoclonal rat antibodies against HA (3F10, ROCHE), at a dilution of 1:10000, and detected with anti-rat immunoglobulin conjugated with horseradish peroxidase using the SuperSignal West Pico Chemiluminescent Substrate (Thermo-Fisher Scientific).

Analysis of Global binding Preference

We downloaded the FASTq files from ZmTB1 and IgG ChIP-seq (Dong et al. 2019). Quality check, mapping and peak calling were conducted on the Galaxy platform (https://usegalaxy.org/) (Afgan et al. 2018). Next, the sequences were mapped using Bowtie 2 setting the mismatches to one. Finally, to identify the peaks we used MACS2. A BED file of the TB1 peaks was produced and intersected with the BED file available from ZmBAD1 DAP-seq (Ricci et al. 2019) to find common targets using BedTools (https://bedtools.readthedocs.io/en/latest/). We analyzed 10kb upstream and 5kb downstream each gene body, extracted from the *Zea mays* v4 genome version. The pipeline for these analyses can be found in **Fig. S14**, see later. In addition, a MEME-ChIP analysis (https://meme-suite.org/meme/tools/meme-chip) was performed with the DAP-seq data of ZmBAD1 to determine its sequence specificity. For this, BedTools was also used to extract the sequence of the peaks from the ZmBAD1 DAP-seq BED file.

Results

Positive selection in the TCP domain contributed to the early diversification of TB1-like proteins in grasses

In order to identify gene duplications within the *TB1-like* clade, we determined the evolutionary history of TCP TFs in the grass family. For a comprehensive and accurate picture of the evolution of *TCP* genes, we incorporated four Monocot species, including *Joinvillea ascendens*, the extant ancestor of Poaceae (McKain et al. 2016). We performed a maximum likelihood (ML) analysis using the translated CDS sequences that recovered the TB1 clade with strong support, and two additional also well-supported subclades, here named BAD1/REP1 and TIG1, also revealing that the latter is a duplication of the first one (**Fig. 1a; Fig. S1a,b**). Interestingly, given that the outgroup species have only TB1 and BAD1 related proteins, but not TIG1, the last subclade emerged as a duplication exclusively restricted to the Poaceae family. Notably, each grass species with a diploid genome has at least one member of each TB1 subclade, including rice or foxtail millet. The only grass species in the tree that despite having also three *TB1-like* genes does not have a TIG1 sequence is barley. Instead, an in-paralog of TB1 appeared in the phylogeny. Expectedly, polyploid species have additional species-specific duplications, like maize and wheat. In maize, we also found a species-specific cluster within the TIG1 clade. In general, within the recovered subclades, species of Pooideae and Panicoideae subfamilies appeared closely related, further supporting the phylogenetic analysis conducted here (**Fig. 1a**).

To investigate the divergence of protein function, we then assessed the molecular evolution within the TB1, BAD1/REP1 and TIG1 subclades of grasses, by constructing an additional ML tree restricted only to TB1-like sequences (**Fig. S1a**). Focusing on the TCP binding domain, the codon-based alignment used in this analysis informed the residue mutations that arose after gene duplication (**Fig. 2a; Fig. S2**), which may be of mechanistic relevance for chromatin binding. Remarkably, positive selection tests found that residues 8, 11, 23, 27 and 34 within the TCP domain are likely to have evolved adaptively (**Fig. 2b; Fig. S2**). In particular, the Asp to Gly mutation at position 23 within the TCP domain that occurred in the TIG1 subclade represents the most radical biochemical change. Interestingly, given that all grass TIG1 sequences contain a Gly in position 23, this mutation likely occurred in the early diversification of the family (**Fig. 2b; Fig. S1a** and **Fig. S2)**. Then, we used the only available crystal structure of a TCP TF (Sun et al. 2020a) to predict possible structural changes conferred by the G23 mutation (**Fig. 2c**). This revealed that the negatively charged Asp exposed outside the TCP domain evolved to a Gly, a smaller and non-charged residue, buried within the domain, most likely affecting the contact region of the TF with the chromatin (**Fig. 2c**). Hence, we selected this residue as a candidate to further explore its potential function in TF chromatin binding activity.

The G23D mutation in ZmTIG1 TCP domain affects its role in branching

The main developmental role of maize *ZmTB1* is the suppression of axillary branching (Doebley et al. 1995). This function is conserved between Monocots and Eu-dicots as revealed by the exacerbated axillary branch number exhibited by *A. thaliana* mutant plants lacking the *TB1* ortholog, *BRANCHED 1* (*BRC1*) (Aguilar-Martínez et al. 2007). A common evo-devo strategy to assess functional conservation is to complement putative ortholog genes in heterologous living systems. Given the functional conservation between *ZmTB1* and *AtBRC1*, we assessed *ZmTB1* ability along with the two paralogs genes *ZmTIG1* and *ZmBAD1*, to revert the branching phenotype of *A. thaliana brc1-2* mutant plants (Aguilar-Martínez et al. 2007). To this end, we stably overexpressed *ZmTB1*, *ZmTIG1* and *ZmBAD1* in the *brc1-2* background (**Fig. 3a,b; Fig. S3a,b**). Expression levels of *TB1*-like genes and protein levels were measured in independent transgenic lines (homozygous T4 generations) to discard differential effects related to mRNA and/or protein abundance (**Fig. S3b,c**) and those with similar levels were used for phenotypic characterization. Two weeks after bolting, branches were counted to explore the potential reversion of *brc1-2* branching phenotype (**Fig. 3a**). As expected, the heterologous expression of *ZmTB1* in the *brc1-2* mutant led to a significant decrease of axillary branch number (**Fig. 3a,b**). Interestingly, *brc1-2* mutant plants expressing *ZmBAD1* showed no reversion of the branching

phenotype and the plants expressing *ZmTIG1* displayed a slight reduction of axillary branches (**Fig. 3a,b**). Altogether, these results highlight the differential ability of maize *TB1*-like genes to resemble BRC1 function in Arabidopsis.

In view of these findings, we wondered if the different axillary branching phenotypes observed in *brc1-2* + ZmTB1 and *brc1-2* + ZmTIG1 Arabidopsis plants could be related to the residue G23 acquired by TIG1 after gene duplication (**Fig. 2a**). Thus, we resurrected Gly23 to Asp residue to obtain *brc1-2* + ZmTIG1-G23D Arabidopsis plants. Remarkably, ZmTIG1-G23D showed an increased capacity to rescue the phenotype of *brc1-2* plants compared to ZmTIG1 and ZmBAD1, closer to the plants expressing ZmTB1 (**Fig. 3a,b**). Interestingly, BRC1 TCP-domain also has an Asp at position 23 (**Fig. S3d**). This strongly suggests that the G23 natural mutation that had arisen in TIG1 alters protein activity, and, therefore, plant development. Altogether, these results suggest that the G23 residue may be involved in the functional divergence of *TB1* paralogs in grasses.

The G23D mutation does not affect ZmTIG1 capacity to form homo and heterodimers

After revealing a biological relevance of the G23D mutation of ZmTIG1, we sought to determine the molecular bases behind the observed phenotypes. TCP TFs bind to chromatin preferentially as homodimers, but can also form heterodimers with other TCPs (Viola et al. 2011). Interestingly, it was shown in the maize B-class MADS-box TF family that a single amino-acid change (Gly/Asp mutation) can turn an obligate heterodimer into a homodimer (Bartlett et al. 2016b). Hence, to determine whether the G23D mutation within the TCP domain of ZmTIG1 impaired its homodimerization, we first tested the interaction ZmTIG1-ZmTIG1 and ZmTIG1-ZmTIG1-G23D by Bimolecular Fluorescence Complementation Assay (BiFC). ZmTIG1 formed homodimers, as expected, and the G23D mutation did not disrupt the homodimerization or the heterodimerization with ZmTB1 and ZmBAD1 (**Fig. 4a; Fig. S4-S10**). In addition, we mutated the Asp residue at position 23 within the TCP domain of ZmTB1 to a Gly residue to test its effect on homodimerization and heterodimerization. As previously observed for the G23D mutation in ZmTIG1, the D23G mutation in ZmTB1 did not affect the ability of ZmTB1 to homodimerize or heterodimerize with ZmTIG1 (**Fig. 4a; Fig. S4-S10**). We further confirmed that the G23D mutation does not affect ZmTIG1 dimerization by performing a co-immunoprecipitation assay (Co-IP). ZmTIG1-GFP or ZmTIG1-G23D-GFP protein fusions were used for anti-GFP immunoprecipitation and ZmTIG1-HA for anti-HA western-blot detection (**Fig. 4b,c**). Given that ZmTIG1-HA was detected after ZmTIG1-GFP and/or ZmTIG1-G23D-GFP immunoprecipitation, we confirmed that this residue does not affect the heterodimer formation (**Fig. 4b,c**). Altogether, these results

indicate that the G23D mutation does not affect the capacity of ZmTIG1 to interact at least with the protein partners tested here. These findings also suggest that another layer of regulation of ZmTIG1 activity may explain the differences of phenotypes previously observed between the *brc1-2* transgenic plant lines (**Fig. 3a,b**).

ZmTIG1 chromatin binding activity is affected by the G23D mutation

The main molecular role of a TF is to bind to chromatin to regulate target gene expression. ZmTB1 is the only TCP member whose chromatin binding sites were identified genome-wide (Dong et al. 2019). To determine if the G23 mutation in the TCP domain of ZmTIG1 affects chromatin binding, we tested the enrichment of ZmTIG1 and ZmTIG1-G23D over five known ZmTB1 direct targets (Dong et al. 2019), by Chromatin Immunoprecipitation assays (ChIP) in maize. To this end, we optimized an Agrobacterium-mediated transient transformation of maize leaves (Zhang et al. 2020). ZmTIG1 and ZmTIG1-G23D were expressed under the control of a constitutive 35S promoter and tagged with GFP for immunoprecipitation and cell localization. To verify that mRNA abundance and protein localization were similar using both constructs we measured transcript levels by RT-qPCR and checked the nuclear protein localization by confocal microscopy (**Fig. S11a,c**). In addition, we measured the GFP signal using fluorimetry to discard differences in protein abundance (**Fig. S11b**). Interestingly, most of the analyzed loci were preferentially bound by ZmTIG1-G23D (**Fig. 5a**). To correlate ZmTIG1 and ZmTIG1-G23D binding activity with gene expression, we measured mRNA expression levels of the five loci. Accordingly, transcript levels were significantly more affected in plants transformed with ZmTIG1-G23D than with ZmTIG1. Although ZmTIG1 ChIP-qPCR do not indicate a differential enrichment of this TF compared to ZmTIG1-G23D over the *ZmTGA1* promoter, we did observed a reduction on the expression levels (**Fig. 5a,b**). Interestingly, despite having an Asp or a Gly at position 23, ZmTIG1 induced *ZmGT1*, *ZmZIM27*, and *ZmRAV*, and repressed *ZmHB33* and *ZmTGA1* expression levels. We also analyzed the effect of ZmTB1 D23G mutation on chromatin binding activity and mRNA levels of the five previous target genes. Notably, the five analyzed loci were preferably bound by the native version of ZmTB1 compared to the mutated one (**Fig. 5c,d; Fig. S12**) and transcripts levels were significantly more affected in plants transformed with ZmTB1 than with ZmTIB1D23G. This differential effect on the mRNA levels probably most relies on the differential binding capacity of the TFs to chromatin.

In rice, *OsEXPA3* and *OsEXPB5* were identified as direct targets of the ZmTIG1 ortholog OsTIG1. Notably, they both contain a TCP binding motif GGNCCC in their promoter region (Zhang et al. 2019). To further understand how the G23D mutation in the TCP domain of ZmTIG1 affects

its activity, we thus tested ZmTIG1 and ZmTIG1-G23D binding to *OsEXPA3* and *OsEXPB5*. For this, rice protoplasts were isolated and transformed either with 35S:ZmTIG1:GFP or 35S:ZmTIG1-G23D:GFP constructs. Protein expression in protoplasts was verified using fluorescence microscopy (**Fig. S13b**), prior proceeding to mRNA quantification and ChIP-qPCR experiments. Potential differences in mRNA levels of *TIG1* and *TIG1-G23D* were discarded through RT-qPCR analyses (**Fig. S13a**). According to the ChIP-qPCR assays, the G23D mutation reduced the ability of ZmTIG1 to recognize *OsEXPA3* and *OsEXPB5* promoters *in vivo* (**Fig. 6a**). Accordingly, *OsEXPA3* and *OsEXPB5* transcript levels were highly incremented in protoplasts transformed with ZmTIG1 compared to ZmTIG1-G23D (**Fig. 6b**), in agreement with the positive role of OsTIG1 reported in the regulation of *OsEXPA3* and *OsEXPB5* transcription (Zhang et al. 2019). Altogether, these results suggest that the G23D mutation mediates chromatin binding preferences across grasses.

The G23D mutation in ZmTIG1 TCP domain also determines the recognition of BRC1 targets in Arabidopsis

We also took advantage of the *brc1-2* + *TB1*-like Arabidopsis lines to establish a mechanistic link between TIG1 chromatin binding capacity and our previous phenotypic observations (**Fig. 3a,b**). To date, only three genes have been identified in *A. thaliana* as directly activated by BRC1, namely the HD-Zip genes *HB21*, *HB40* and *HB53* (Gonzalez-Grandio et al. 2017). To assess if this regulatory module is indeed responsible for the different complementation observed in *brc1-2* + ZmTIG1 and *brc1-2* + ZmTIG1-G23D plants, we evaluated whether *HB21/40/53* are also differentially bound by ZmTIG1. ChIP-qPCR experiments performed in the *brc1-2* + *TB1*-like Arabidopsis lines showed that the three HD-Zip genes are direct targets of ZmTIG1-G23D, while ZmTIG1 binds to *HB40* and *HB53* to a lesser extent (**Fig. 7a**). Remarkably, the expression level of *HB21/40/53* was slightly induced in *brc1-2* + ZmTIG1 plant lines, but was strongly up-regulated in *brc1-2* + ZmTIG1-G23D plants where the amino acid under scrutiny mimics the BRC1 DNA binding domain (**Fig. 7b**). These results further indicate that the branching phenotypes previously observed (**Fig. 3a-b**) correlate with the expression levels of *BRC1* target genes.

Grass TB1-like genes directly regulate different sets of genes albeit sharing the same sequence specificity

TCP class II TFs are well-known for binding to site II elements "GGNCCC" (Kosugi and Ohashi 2002). Thus, we searched for a possible difference in sequence specificity within maize TB1-like TFs. Global binding preferences of ZmTB1 were recently identified by ChIP-seq, confirming its expected sequence specificity for GGNCCC elements (Dong et al. 2019). Additionally, we used the publicly available datasets for ZmBAD1 DAP-seq assay (Ricci et al. 2019) and performed a MEME-ChIP analysis to obtain its global sequence preference. This analysis also returned a highly similar element indicating that ZmTB1 and ZmBAD1 share the same sequence specificity (**Fig. S14**), as expected. No global data is available for any TIG1 grass TF yet. Nevertheless, a recent study of TIG1 in rice indicates that it recognizes the canonical GGNCCC element of their three direct targets, as revealed by ChIP-qPCR (Zhang et al. 2019). Altogether, these informations suggest that there is no difference in sequence specificity between *TB1-like* genes in maize.

We also intersected bound peaks of ZmTB1 and ZmBAD1 in order to evaluate to what extent they bind common targets across the maize genome. By analyzing 10kb upstream and 5kb downstream from each gene body, 4175 and 7314 sites were found as bound by BAD1 and TB1 respectively. Remarkably, only 269 peaks emerged as common targets of both TFs. This overlap of peaks was smaller than expected by chance, according to a Fisher test (odds ratio 0,39; p value $9{,}8 \times 10^{-62}$), meaning that BAD1 and TB1 have different target preferences in spite of sharing the same sequence specificity (**Fig. S14b,c**).

Discussion

TFs have a pervasive history of gene duplications in plants (Panchy et al. 2016). However, the mechanism underlying how duplicated plant TFs evolve to bind different target genes remains unclear. Hence, in this work, we tackled how paralog TFs diversify their functions through the incorporation of novel residues that modulate their chromatin binding preferences, and therein, gene direct target expression regulation. By analyzing the molecular evolution of the TB1 clade of TCP TFs in grasses, we identified a grass specific paralog subclade, TIG1, which shows signals of adaptive evolution within the DNA binding domain. We investigated the molecular and functional effect of the most radical residue incorporated after gene duplication, an Asp to Gly at position 23 of the TCP domain. We uncovered that this mutation led the path to neo-functionalization of the TIG1 subclade in grasses through the modulation of chromatin binding activity, impacting target gene expression and final plant architecture (Fig. 8).

Evolution of TB1-like genes in grasses

According to our phylogenetic analyses of TCP TFs, TB1 and BAD1 subclades are present in the whole order Poales. Interestingly, TIG1 sequences are only present in species restricted to Poaceae, indicating that this is an exclusive duplication event. The placement of the TIG1 subclade as an exclusive paralog within the grasses is consistent with a previous phylogeny of TB1 genes in monocots (González-Grándio and Cubas, 2016). Given that all grass species have conserved the *TIG1* sequence alongside *TB1* and *BAD1*, this highlights that this exclusive subclade is functionally relevant. In agreement with a previous report (Poursarebani et al. 2020), the lack of *TIG1* sequence in barley is exceptional.

Maize plants having deregulated levels of *ZmTB1* or point mutations in ZmBAD1 exhibit a different plant architecture. Increased levels of *TB1* drastically reduce axillary branching in the domesticated maize from teosinte (Doebley et al. 1997), while mutations of residue 9 or 21 within the ZmBAD1 TCP domain alters the inflorescence angle (Bai et al. 2012). Although the biological function of *ZmTIG1* has not been described so far, rice plants with deregulated *OsTIG1* display altered tiller angle (Zhang et al. 2019), a phenotype which resembles the altered angle of lateral branches in maize *bad1-1* and *bad1-2* (Bai et al. 2012). In addition, *ZmTIG1* is expressed in developing inflorescence primordia suggesting that it is fully functional. On the other hand, the expression of *ZmTIG1* and *ZmBAD1* in inflorescence primordia and in kernels appears to show complementary expression patterns (**Fig. S15**). Taken together, these pieces of information suggest that despite being paralogs, *ZmTIG1* and *ZmBAD1* are most likely not redundant. Further experimentation is thus needed to test this hypothesis.

Several paths can occur after gene duplication, like gene sub-functionalization or neo-functionalization (Ohno 1970). For instance, in the first scenario, gene duplicates conserve the original function. On the contrary, the second scenario occurs when novel functions are acquired by paralog genes (Ohno 1970). Broad surveys of *TB1-like* genes in several grass species revealed that gene expression deregulation or protein activity alteration of any of them can severely affect plant development and architecture (Doebley et al. 1995; Yuan et al. 2009; Minakuchi et al. 2010; Ramsay et al. 2011; Bai et al. 2012; Dixon et al. 2018; Zhang et al. 2019; Lyu et al. 2020; Poursarebani et al. 2020), It was recently reported that rice *OsTb1* and its closest paralog *OsTb2/REP1* showed opposite functions in inflorescence development, revealing contrasting modes of action between *TB1* paralogs in rice (Lyu et al. 2020). This suggests that neo-functionalization is one of the probable paths between some *TB1* paralogs in Poaceae.

D23G acquired by adaptive selection in TIG1 modulates protein activity far-reaching developmental outputs

Plant complementation phenotype experiments in *brc1-2* Arabidopsis mutants informed that ZmTB1 has an outstanding capacity to suppress axillary branching, compared to ZmBAD1 and ZmTIG1. When we introduced the Asp residue in ZmTIG1 to resemble ZmTB1 TCP domain, the axillary branches were further repressed accordingly. Moreover, rice *fc1-2* null allele (here OsTIG1) has an increased tiller number (Minakuchi et al. 2010). Remarkably, *fc1-2* plants exhibit a deletion of 9 residues within the TCP domain, starting from Asp 23. This further indicates that this region of the TCP domain where Asp 23 is located is crucial for TB1-like protein activity and plant development (Minakuchi et al. 2010). Despite naturally having the Asp at position 23, ZmBAD1 showed no capacity to rescue the phenotype of *brc1-2* plants. Although this observation somehow contradicts the potential relevance of this residue, it should be noticed that ZmBAD1 and ZmTIG1 also have several different additional residues within and outside the TCP domain that may explain their differential ability to repress axillary branches in *brc1-2* plants. Moreover, as mentioned above, maize *bad1-1* and *bad1-2* plants showed impaired activity of ZmBAD1 due to single mutations of other residues within the DNA binding domain (Bai et al. 2012). Altogether, it can be argued that in the particular case of ZmBAD1 other relevant residues might be obscuring the importance of Asp 23 revealed here. Considering the implications that natural mutations can imprint on grass *TB1* paralogs, also notice that *OsTb1* and *OsTb2/REP1* have opposite roles in inflorescence development despite being closely related (Lyu et al. 2020). Given that *OsTb2* (which belongs to the BAD1 clade) has neo-functionalized to induce tillering in rice (Lyu et al. 2020), the lack of complementation in *brc1-2* + ZmBAD1 plants agrees with this finding.

Adaptive evolution dictates chromatin binding preference differences between TB1-like TCP TFs in grasses

Considering that the phenotype of plants transformed with ZmTIG1 or ZmTIG1-G23D revealed the importance of the G23 mutation, we sought to determine what features of the protein activity were involved in the process. A previous study reported that a single Asp to Gly fixed by positive selection can affect the dimerization of MADS-box TFs within Poales affecting plant development (Bartlett et al. 2016a), so here we initially expected a similar effect. Nevertheless, we found that this mutation has no impact on homodimer or heterodimer formation. Based on structural information, the position 23 of the TCP domain is in close proximity with the contact region with the DNA (Sun et al. 2020a). Altogether, the evidence suggested that this mutation is involved in a molecular function other than dimerization activity.

By testing the impact of the G23D mutation by analyzing several targets in maize, rice and Arabidopsis, we revealed that indeed this residue modulates the chromatin binding preference of

this TF. The ChIP assays performed on five ZmTB1 direct targets showed that ZmTIG1 is differentially enriched over the promoter of these loci when we introduce an Asp at position 23 in the TCP domain. Notably, given that ZmTB1 naturally carries the Asp in position 23, the native version of this TF exhibits higher enrichment over these loci compared to the mutated version. Accordingly, mRNA transcription levels of all the analyzed genes were more affected by ZmTB1 and ZmTIG1-G23D proteins compared to ZmTB1-D23G and ZmTIG1. Altogether, these results further support the relevance of the 23 position in the TCP domain for the modulation of chromatin binding preference. Interestingly, ZmTIG1-G23D and ZmTIG1 increased the transcription of only three of the TB1 direct targets analyzed (*ZmGT1*, *ZmZIM27*, and *ZmRAV*). This is in agreement with the known ZmTB1 positive effect on the transcription of these genes (Dong et al. 2019). Unexpectedly, the expression analyses here revealed that ZmTIG1-G23D repressed the transcription of *HB33* and *TGA*. Therefore, these results imply that although ZmTIG1-G23D performs better than ZmTIG1 to bind ZmTB1 targets as expected, the transcriptional output of this differential binding is more complex than initially assumed. Most likely, other mutations within or outside the TCP domain of ZmTIG1 may turn this TF into a repressor of these particular loci, either by affecting protein-protein and/or protein-chromatin interaction. Yet, despite the positive or negative role showed by ZmTIG1 on the transcription of TB1-target loci, the G23D mutation always exerted the strongest effect. Moreover, given that OsTb1 and OsTb2/REP1 have opposite roles in rice tillering, it is expected that this different behavior between TB1 paralogs also entails an alternative mode of action at the molecular level. On the other hand, rice TIG1 targets evaluated were preferentially bound by wild type ZmTIG1 compared to the mutated version, as expected. Clearly, the Gly at position 23 favors the binding to *OsEXPA3* and *OsEXPB5* promoters inducing their expression. More evidence about the impact of G23D mutation on the chromatin binding preference of target genes was provided by the ChIP assays performed over HD-Zip direct target genes of BRC1 in Arabidopsis. Although ZmTIG1 showed some enrichment over *AtHB40* and *AtHB53*, the introduction of the Asp 23 resembling BRC1 DNA binding domain boosted chromatin binding of the three HD-Zip genes tested. In addition, mRNA levels of these genes were incremented accordingly. To sum up, these results confirm that the G23D mutation fixed by positive selection in the grass TIG1 clade affects protein activity impacting on chromatin binding preference of target genes.

The ChIP-seq of ZmTB1 and the DAP-seq of ZmBAD1 experiments revealed a highly similar sequence preference (Dong et al. 2019; Ricci et al. 2019). Although conceptual (*in vivo* vs *in vitro* assay) and technical (different tissue samples) differences between a ChIP-seq and a DAP-seq experiment should be take it into account, yet, our global analyses revealed that they

share only a small fraction of direct targets. In addition, direct targets of rice TIG1 contain a GGNCCC element in the respective promoter sequences used to test the TF-chromatin interaction (Zhang et al. 2019). This indicates a highly similar sequence affinity between grass TB1 paralogs. In addition, the sequence specificity of the TCP family is highly conserved since early diverging land plants (Karaaslan et al. 2020). ZmTB1 and ZmBAD1 recognized the same *cis*-element, but still, they directly control a highly different set of targets, implying that additional features beyond sequence specificity are crucial to determine chromatin preference. Hence, this prompts to find other chromatin features to explain how TCP TFs define their binding preferences. In this sense, it has been demonstrated that particularly TCP TFs have a role in chromatin architecture. Notably, self-interacting genomic regions known as topologically associated domains (TADs) were identified in rice and maize revealing an enrichment of *cis*-elements recognized by TCP proteins (Liu et al. 2017; Y. Sun et al. 2020b). In addition, in *Marchantia polymorpha*, TADs were found to be decorated with MpTCP1 at the borders revealing the first known association of a plant TF with special chromatin-packing modules (Karaaslan et al. 2020). Moreover, the expression of genes located in MpTCP1-rich TADs is differentially affected in the absence of *MpTCP1*, indicating a relevant role for gene transcription in this space. What other features of the chromatin are being preferred by different TCP TFs to finally define its targets would probably become an important endeavor in the following years. Here, analyzing the chromatin status through data obtained from available ATAC-seq experiments from maize, we found that all the ZmTB1 direct targets here tested overlap with open chromatin regions (Fig. S17). On the contrary, the bound regions of the three known direct targets of OsTIG1 in rice do not (Zhang et al. 2019), suggesting that this TF can invade chromatin regions that are not necessarily relaxed (Fig. S16). To unveil if TIG1 behaves as a pioneer TF after the acquisition of an Asp at position 23 further research at global scale will be required. Certainly, this hypothesis does not rule out the possibility that other features of the chromatin are of relevance to utterly determine the distinct binding preferences between this or other paralog TFs.

Here we provide compelling evidence that after a drastic physicochemical change produced by the fixation of a residue in a relevant functional domain, TFs can evolve through diversifying its chromatin binding preference. Remarkably, this work opens new avenues to study the mechanistic basis behind the evolution of chromatin binding preferences of duplicated TFs.

Acknowledgements

We thank Virginia Miguel for kindly provide the clones of HaHB11, and Unidad de Mejoramiento Vegetal from IAL (CONICET-UNL) for *Z. mays* B73 and *O. sativa* Kitaake seeds. This work was supported by Agencia Nacional de Promoción de la Investigación, el Desarrollo Tecnológico y la Innovación (ANPCyT) (PICT-2019-00034, PICT-2019-04137, PICT-2020-00218). N.M. is a fellow of ANPCyT.

Author Contributions

L.L. conceived the original concept. L.L. designed the experiments and oversaw the project and analyses. L.L. and F.A. acquired fundings. N.M. and L.L. performed the experiments. C.F.-F. assisted in sample preparation. N.M., F.A and C.F.-F. contributed to the interpretation and presentation of the results in the main manuscript and supplementary documents. L.L. wrote the manuscript with input from all the authors.

Data Availability

The data that support the findings of this study are available from the corresponding author upon reasonable request.

Competing Interests

None declared.

References

Afgan E, Baker D, Batut B, Van Den Beek M, Bouvier D, Ech M, Chilton J, Clements D, Coraor N, Grüning BA, et al. 2018. The Galaxy platform for accessible, reproducible and collaborative biomedical analyses: 2018 update. *Nucleic Acids Res.* 46: 537–544.

Aggarwal P, Das Gupta M, Joseph AP, Chatterjee N, Srinivasan N, Nath U. 2010. Identification of Specific DNA Binding Residues in the TCP Family of Transcription Factors in *Arabidopsis*. *Plant Cell* 22: 1174–1189.

Aguilar-Martínez JA, Poza-Carrión C, Cubas P. 2007. Arabidopsis Branched1 acts as an integrator of branching signals within axillary buds. *Plant Cell* 19: 458–472.

Bai F, Reinheimer R, Durantini D, Kellogg EA, Schmidt RJ. 2012. TCP transcription factor, BRANCH ANGLE DEFECTIVE 1 (BAD1), is required for normal tassel branch angle formation in maize. *Proc. Natl. Acad. Sci. U. S. A.* 109: 12225–12230.

Bartlett M, Thompson B, Brabazon H, Del Gizzi R, Zhang T, Whipple C. 2016a. Evolutionary Dynamics of Floral Homeotic Transcription Factor Protein-Protein Interactions. *Mol. Biol. Evol.* 33: 1486–1501.

Bartlett M, Thompson B, Brabazon H, Del Gizzi R, Zhang T, Whipple C. 2016b. Evolutionary Dynamics of Floral Homeotic Transcription Factor Protein-Protein Interactions. *Mol. Biol. Evol.* 33: 1486–1501.

Borba AR, Serra TS, Górska A, Gouveia P, Cordeiro AM, Reyna-Llorens I, Kneřová J, Barros PM, Abreu IA, Oliveira MM, et al. 2018. Synergistic binding of bHLH transcription factors to the promoter of the maize NADP-ME gene used in C4 photosynthesis is based on an ancient code found in the ancestral C3 state. *Mol. Biol. Evol.* 35: 1690–1705.

Busch A, Deckena M, Almeida-Trapp M, Kopischke S, Kock C, Schüssler E, Tsiantis M, Mithöfer A, Zachgo S. 2019. MpTCP1 controls cell proliferation and redox processes in Marchantia polymorpha. *New Phytol.* 224: 1627–1641.

Conant GC, Wolfe KH. 2008. Turning a hobby into a job: How duplicated genes find new functions. *Nat. Rev. Genet.* 9: 938–950.

Cubas P, Lauter N, Doebley J, Coen E, Centre JI, Lane C, Nr N. 1999. The TCP domain : a motif found in proteins regulating plant growth and development. *T Plant J.* 18:215–222.

Derbyshire MC, Harper LA, Lopez-Ruiz FJ. 2021. Positive Selection of Transcription Factors Is a Prominent Feature of the Evolution of a Plant Pathogenic Genus Originating in the Miocene. *Genome Biol. Evol.* 13: 1–19.

Dixon LE, Greenwood JR, Bencivenga S, Zhang P, Cockram J, Mellers G, Ramm K, Cavanagh C, Swain SM, Boden SA. 2018. TEOSINTE BRANCHED1 regulates inflorescence architecture and development in bread wheat (*Triticum aestivum*). *Plant Cell* 30: 563–581.

Doebley J, Stec A, Gustus C. 1995. teosinte branched1 and the origin of maize: Evidence for epistasis and the evolution of dominance. *Genetics* 141: 333–346.

Doebley J, Stec A, Hubbard L. 1997. The evolution of apical dominance in maize. *Nature* 386: 485–488.

Dong Z, Xiao Y, Govindarajulu R, Feil R, Siddoway ML, Nielsen T, Lunn JE, Hawkins J, Whipple C, Chuck G. 2019. The regulatory landscape of a core maize domestication

module controlling bud dormancy and growth repression. *Nat. Commun.* 10, 3810.

Edgar RC. 2004. MUSCLE: Multiple sequence alignment with high accuracy and high throughput. *Nucleic Acids Res.* 32: 1792–1797.

Gonzalez-Grandio E, Pajoro A, Franco-Zorrilla JM, Tarancon C, Immink RGH, Cubas P. 2017. Abscisic acid signaling is controlled by a BRANCHED1/HD-ZIP cascade in Arabidopsis axillary buds. *Proc. Natl. Acad. Sci. U. S. A.* 114: 245–254.

Gübitz T, Caldwell A, Hudson A. 2003. Rapid molecular evolution of CYCLOIDEA-like genes in antirrhinum and its relatives. *Mol. Biol. Evol.* 20: 1537–1544.

He, F., Chen, S., Ning, Y. and Wang, G.-L. 2016. Rice (Oryza sativa) protoplast isolation and its application for transient expression analysis. *Curr. Protoc. Plant Biol.* 1: 373-383.

Hughes TE, Langdale JA, Kelly S. 2014. The impact of widespread regulatory neofunctionalization on homeolog gene evolution following whole-genome duplication in maize. *Genome Res.* 24: 1348–1355.

Igartua E, Contreras-Moreira B, Casas AM. 2020. TB1: From domestication gene to tool for many trades. *J. Exp. Bot.* 71: 4621–4624.

Kalyaanamoorthy S, Minh BQ, Wong TKF, Von Haeseler A, Jermiin LS. 2017. ModelFinder: Fast model selection for accurate phylogenetic estimates. *Nat. Methods* 14: 587–589.

Karaaslan ES, Wang N, Faiß N, Liang Y, Montgomery SA, Laubinger S, Berendzen KW, Berger F, Breuninger H, Liu C. 2020. Marchantia TCP transcription factor activity correlates with three-dimensional chromatin structure. *Nat. Plants* 6: 1250–1261.

Kosugi S, Ohashi Y. 1997. PCF1 and PCF2 specifically bind to cis elements in the rice proliferating cell nuclear antigen gene. *Plant Cell* 9: 1607–1619.

Kosugi S, Ohashi Y. 2002. DNA binding and dimerization speci ® city and potential targets for the TCP protein family. *Plant J.* 30 (3):337-48.

Kumar S, Stecher G, Li M, Knyaz C, Tamura K. 2018. MEGA X: Molecular evolutionary genetics analysis across computing platforms. *Mol. Biol. Evol.* 35: 1547–1549.

Lai X, Chahtane H, Martin-arevalillo R, Zubieta C, Lai X, Chahtane H, Martin-arevalillo R, Zubieta C, Contrasted FP. 2020. Contrasted evolutionary trajectories of plant transcription factors. *Current Opinion in Plant Biology*. 54: 101-107.

Lee JH, Jin S, Young Kim S, Kim W, Ahn JH. 2017. A fast, eficient chromatin immunoprecipitation method for studying protein-DNA binding in Arabidopsis mesophyll protoplasts. *Plant methods*. 13, 42.

Lewis JM, Mackintosh CA, Shin S, Gilding E, Kravchenko S, Baldridge G, Zeyen R, Muehlbauer GJ. 2008. Overexpression of the maize Teosinte Branched1 gene in wheat suppresses tiller development. *Plant Cell Rep.* 27: 1217–1225.

Lin R-C, Rausher MD. 2021a. Ancient Gene Duplications, Rather Than Polyploidization, Facilitate Diversification of Petal Pigmentation Patterns in Clarkia gracilis (Onagraceae) . *Mol. Biol. Evol.* 38: 5528–5538.

Lin R-C, Rausher MD. 2021b. R2R3-MYB genes control petal pigmentation patterning in Clarkia gracilis ssp. sonomensis (Onagraceae). *New Phytol.* 229: 1147–1162.

Liu C, Cheng Y-J, Wang J-W, Weigel D. 2017. Prominent topologically associated domains differentiate global chromatin packing in rice from Arabidopsis. *Nat. Plants* 3: 742-748.

Luo D, Carpenter R, Vincent C, Copsey L, Coen E. 1996. Origin of floral asymmetry in Antirrhinum. *Nature* 383: 794–799.

Lyu J, Huang L, Zhang S, Zhang Y, He W, Zeng P, Zeng Y, Huang G, Zhang J, Ning M, et al. 2020. Neo-functionalization of a Teosinte branched 1 homologue mediates adaptations of upland rice. *Nat. Commun.* 11: 1–13.

Martín-Trillo M, Grandío EG, Serra F, Marcel F, Rodríguez-Buey ML, Schmitz G, Theres K, Bendahmane A, Dopazo H, Cubas P. 2011. Role of tomato BRANCHED1-like genes in the control of shoot branching. *Plant J.* 67: 701–714.

Nicholas M and Cubas P. 2016. TCP Transcription Factors: Evolution, Structure, and Biochemical Function. In: Daniel Gonzalez, editor. PLANT TRANSCRIPTION FACTORS. Elsevier. p139-151.

de Meaux J. 2018. Cis-regulatory variation in plant genomes and the impact of natural selection. *Am. J. Bot.* 105: 1788–1791.

Minakuchi K, Kameoka H, Yasuno N, Umehara M, Luo L, Kobayashi K, Hanada A, Ueno K, Asami T, Yamaguchi S, et al. 2010. FINE CULM1 (FC1) works downstream of strigolactones to inhibit the outgrowth of axillary buds in rice. *Plant Cell Physiol.* 51: 1127–1135.

Moison M, Martínez Pacheco J, Lucero L, Fonouni-Farde C, Rodríguez-Melo J, Mansilla N, Christ A, Bazin J, Benhamed M, Ibañez F, Crespi M, Estevez JM, Ariel F. 2021. The lncRNA APOLO interacts with the transcription factor WRKY42 to trigger root hair cell expansion in response to cold. *Mol. Plant*. 14: 1–12.

Navaud O, Dabos P, Carnus E, Tremousaygue D, Hervé C. 2007. TCP transcription factors predate the emergence of land plants. *J. Mol. Evol.* 65: 23–33.

Nguyen LT, Schmidt HA, Von Haeseler A, Minh BQ. 2015. IQ-TREE: A fast and effective stochastic algorithm for estimating maximum-likelihood phylogenies. *Mol. Biol. Evol.* 32: 268–274.

Nicolas M, Cubas P. 2016. TCP factors: New kids on the signaling block. *Curr. Opin. Plant Biol.* 33:33–41.

Ohno S. 1970. Evolution by Gene Duplication. New York, Heidelberg, Berlin: Springer-Verlag.

Panchy N, Lehti-Shiu M, Shiu SH. 2016. Evolution of gene duplication in plants. *Plant Physiol.* 171: 2294–2316.

Poursarebani N, Trautewig C, Melzer M, Nussbaumer T, Lundqvist U, Rutten T, Schmutzer T, Brandt R, Himmelbach A, Altschmied L, et al. 2020. COMPOSITUM 1 contributes to the architectural simplification of barley inflorescence via meristem identity signals. *Nat. Commun.* 11, 5138.

Ramsay L, Comadran J, Druka A, Marshall DF, Thomas WTB, MacAulay M, MacKenzie K, Simpson C, Fuller J, Bonar N, et al. 2011. INTERMEDIUM-C, a modifier of lateral spikelet fertility in barley, is an ortholog of the maize domestication gene TEOSINTE BRANCHED 1. *Nat. Genet.* 43: 169–172.

Ricci WA, Lu Z, Ji L, Marand AP, Ethridge CL, Murphy NG, Noshay JM, Galli M, Mejía-Guerra MK, Colomé-Tatché M, et al. 2019. Widespread long-range cis-regulatory elements in the maize genome. *Nat. Plants* 5: 1237–1249.

Schindelin J, Arganda-Carreras I, Frise E, Kaynig V, Longair M, et al. 2013. Fiji: an Open Source platform for biological image analysis. *Nat Methods*. 9(7): 676–682.

Sun L, Zou X, Jiang M, Wu X, Chen Y, Wang Qianchao, Wang Qin, Chen L, Wu Y. 2020a. The crystal structure of the TCP domain of PCF6 in Oryza sativa L. reveals an RHH-like fold. *FEBS Lett.* 594: 1296–1306.

Sun Y, Dong L, Zhang Y, Lin D, Xu W, Ke C, Han L, Deng L, Li G, Jackson D, et al. 2020b. 3D genome architecture coordinates trans and cis regulation of differentially expressed ear and tassel genes in maize. *Genome Biol.* 21: 1–25.

Takeda T, Suwa Y, Suzuki M, Kitano H, Ueguchi-Tanaka M, Ashikari M, Matsuoka M, Ueguchi C. 2003. The OsTB1 gene negatively regulates lateral branching in rice. *Plant J.* 33: 513–520.

Uberti Manassero NG, Viola IL, Welchen E, Gonzalez DH. 2013. TCP transcription factors: Architectures of plant form. *Biomol. Concepts* 4: 111–127.

Viola IL, Reinheimers R, Ripoll R, Uberti Manassero NG, Gonzalez DH. 2012. Determinants of the DNA binding specificity of class I and class II TCP transcription factors. *J. Biol. Chem.* 287: 347–356.

Viola IL, Uberti Manassero NG, Ripoll R, Gonzalez DH. 2011. The Arabidopsis class I TCP transcription factor AtTCP11 is a developmental regulator with distinct DNA-binding properties due to the presence of a threonine residue at position 15 of the TCP domain. *Biochem. J.* 435: 143–155.

Wang H, Studer AJ, Zhao Q, Meeley R, Doebley JF. 2015. Evidence that the origin of naked kernels during maize domestication was caused by a single amino acid substitution in tga1. *Genetics* 200: 965–974.

Wang Z, Yang L, Wu D, Zhang N, Hua J. 2021. Polymorphisms in cis-elements confer SAUR26 gene expression difference for thermo-response natural variation in Arabidopsis. *New Phytol.* 229: 2751–2764.

Wu N, Zhu Y, Song W, Li Y, Yan Y, Hu Y. 2014. Unusual tandem expansion and positive selection in subgroups of the plant GRAS transcription factor superfamily. *BMC Plant Biol.* 14: 1–21.

Yuan Z, Gao S, Xue D-W, Luo D, Li L-T, Ding S-Y, Yao X, Wilson Z a, Qian Q, Zhang D-B. 2009. RETARDED PALEA1 controls palea development and floral zygomorphy in rice. *Plant Physiol.* 149: 235–244.

Zhang W, Tan L, Sun H, Zhao X, Liu F, Cai H, Fu Y, Sun X, Gu P, Zhu Z, et al. 2019. Natural Variations at TIG1 Encoding a TCP Transcription Factor Contribute to Plant Architecture Domestication in Rice. *Mol. Plant* 12: 1075–1089.

Zhang Y, Chen M, Siemiatkowska B, Rey Toleco M, Jing Y, Strotmann V, Zhang J, Stahl Y, Fernie A. 2020. A Highly Efficient Agrobacterium-Mediated Method for Transient Gene Expression and Functional Studies in Multiple Plant Species. *Plant Comm*. 1, 100028.

Zhang WM, Fang D, Cheng XZ, Cao J, Tan XL. 2021. Insights Into the Molecular Evolution of AT-Hook Motif Nuclear Localization Genes in *Brassica napus*. *Front. Plant Sci.* 12, 714305.

Figure legends

Figure 1. Phylogeny of TCP TFs in Poales. Genome-wide maximum likelihood tree of TCP proteins in Monocots obtained with IQTREE2. The TB1 clade was enlarged for a better visualization. Species names and their corresponding sequence identifiers were depicted in the same color. The asterisk indicates a species-specific clade of *Z. mays* within the grass-specific TIG1 subclade. Support values are indicated by the color of the branches. Gene names of functionally characterized TB1 genes in grasses are indicated with their references.

Figure 2. Molecular evolution of the TB1 clade in Poales. A) Alignment of the TCP domain of the three TB1 members of maize (ZmTB1: AC233950.1_FG002; ZmBAD1: GRMZM2G110242; ZmTIG1: GRMZM2G060319), and OsPCF6 of rice. The two α-helix and β-strands are marked according to the ribbon helix-helix structure of the TCP domain (Sun et al 2020a). The Asp to Gly mutation at position 23 in ZmTIG1 is marked with a light-blue box. B) Weblogo of the TCP domain of the three TB1 clades depicted over the condensed tree of Fig. S1. Residues under positive selection (ω > 1) are marked with a black arrow, and with a red arrow the residue at position 23. C) Structure overview of the TCP domain of ZmTIG1 and ZmTIG1 with the Asp resurrected at position 23 within the α1. Models were obtained with SWISSMODEL (https://swissmodel.expasy.org) using the crystal structure of OsPCF6 as a template (PDB: 5ZKT). Cartoons were prepared with PyMOL (https://pymol.org).

Figure 3. Heterologous expression of *ZmTB1* genes in Arabidopsis results in a differential rescue of the branching number of the *brc1-2* mutant plants. A) Violin plots showing the branch number of the transgenic Arabidopsis plants constitutively expressing *ZmTB1*, *ZmBAD1*, *ZmTIG1* or *ZmTIG1-G23D* in the *brc1-2* background, registered two weeks after bolting. Three different homozygous lines were analyzed per construct (n > 22). Asterisks denote significant differences among means (ANOVA). B) Plant architecture of representative lines of each construct used to complement the *brc1-2* mutant.

Figure 4. Analysis of G23D within ZmTIG1 mutation on dimer formation. A) Protein interaction assayed by BiFC experiment in *N. benthamiana* leaves transiently co-transformed with

different constructs fused either to N- and C-terminal YFP domains. B) and C) Co-immunoprecipitation of ZmTIG1 and ZmTIG1-G23D using isolated nuclei of *N. benthamiana* leaves transiently transformed. The Ponceau staining served as a loading control.

Figure 5. *In vivo* analysis of the impact of G23D mutation within ZmTIG1 on the chromatin binding preference. A) ChIP-qPCR assay of ZmTB1 targets (as identified by Dong et al. 2019) using WT maize leaves Agrobacterium-mediated transiently transformed with *ZmTIG1* or *ZmTIG1-G23D*. Probes over the *ZmActin* locus were used as a negative control. The results indicate the level of immunoprecipitated chromatin with anti-GFP relative to anti-IgG (negative control). B) Relative transcript levels measured by RT-qPCR in maize leaves transformed with *ZmTIG1* or *ZmTIG1-G23D*. C) ChIP-qPCR assay of *ZmTB1* or *ZmTB1-D23G* using WT maize leaves transiently transformed with *ZmTB1-GFP* or *ZmTB1-D23G-GFP*. D) Relative transcript levels measured by RT-qPCR in maize leaves transformed with *ZmTB1* or *ZmTB1-D23G*. Bars represent the average ± SD of three technical replicates in (A) and (C) and three biological replicates in (B) and (D). * p<0,05, two-tailed Student's *t*-test. n.d. means not detected.

Figure 6. A) ChIP-qPCR assay of OsFC1 targets (obtained from Zhang et al. 2019) using rice protoplast transiently transformed with *ZmTIG1* or *ZmTIG1-G23D*, expressed as in (A). *OsActin* probes were used as a negative control. B) *EXPA3* and *EXPB5* relative transcript levels measured by RT-qPCR. Bars represent the average ± SD of three technical replicates in (A), and three biological replicates in (B). * p<0,05, two-tailed Student's *t*-test.

Figure 7. G23D mutation within ZmTIG1 resembles AtBRC1 mode of action. A) Immunoprecipitation of BRC1 targets (as identified by Gonzalez-Grandío et al. 2019) using anti-GFP on stable Arabidopsis plant lines transformed with *ZmTIG1* (line #4) or *ZmTIG1-G23D* (line #5). *AtActin* probes were used as a negative control. The results were expressed as in previous ChIP experiments. B) Relative transcript levels of BRC1 targets in *brc1-2+ZmTIG1* or *brc1-2+ZmTIG1-G23D* complemented plants measured by RT-qPCR. Bars represent the average ± SD of three technical replicates in (A), and three biological replicates in (B). * p<0,05, two-tailed Student's *t*-test.

Figure 8. The hypothesis of TB1 clade evolution in grasses. The TIG1 paralog subclade emerged in Poaceae being exclusive for this family. An Asp to Gly mutation at position 23 of the TCP domain occurred early in the diversification of the Poaceae (Fig. 2; Fig. S2). This mutation affects chromatin binding preference and transcriptional outputs.

Supplementary Information

Additional supporting information may be found in the online version of this article.

Fig. S1. Phylogenetic analysis and selection test of *TB1-like* genes in Poales.

Fig. S2. TCP DNA binding domain depicted alongside each sequence over the ML tree of *TB1-like* genes of Poales.

Fig. S3. Heterologous expression of *TB1-like Z. mays* genes in Arabidopsis.

Fig. S4. Additional controls of the BiFC assay of HaHB11 in *N. benthamiana* leaves.

Fig. S5. Additional controls of the BiFC assay of ZmTIG1 in *N. benthamiana* leaves.

Fig. S6. Additional controls of the BiFC assay of ZmTIG1-G23D in *N. benthamiana* leaves.

Fig. S7. Additional controls of the BiFC assay of ZmTB1 in *N. benthamiana* leaves.

Fig. S8. Additional controls of the BiFC assay of ZmTB1-D23G in *N. benthamiana* leaves.

Fig. S9. Additional controls of the BiFC assay of ZmBAD1 in *N. benthamiana* leaves.

Fig. S10. Quantification of the BiFC experiments of Fig. 4A and FigS4-S9.

Fig. S11. Transiently transformed Maize B73 first and second leaves with TIG1 and TIG1-G23D.

Fig. S12. Transiently transformed Maize B73 first and second leaves with TB1 and TB1-D23G.

Fig. S13. Transiently transformed rice protoplast.

Fig. S14. Genome-wide analysis of ZmTB1 and ZmBAD1 binding preference.

Fig. S15. Expression pattern of *ZmTIG1* and *ZmBAD1* in maize tassel and ear inflorescence primordia and in kernels.

Fig. S16. Chromatin profile of ZmTIG1 direct targets in rice.

Fig. S17. Chromatin profile of ZmTB1 direct targets in maize.

Table S1. List of the species used for the phylogenetic analyses and gene ID of the TB1 clade.

Table S2. Clones used for biochemical and functional experiments.

Table S3. Primer list.

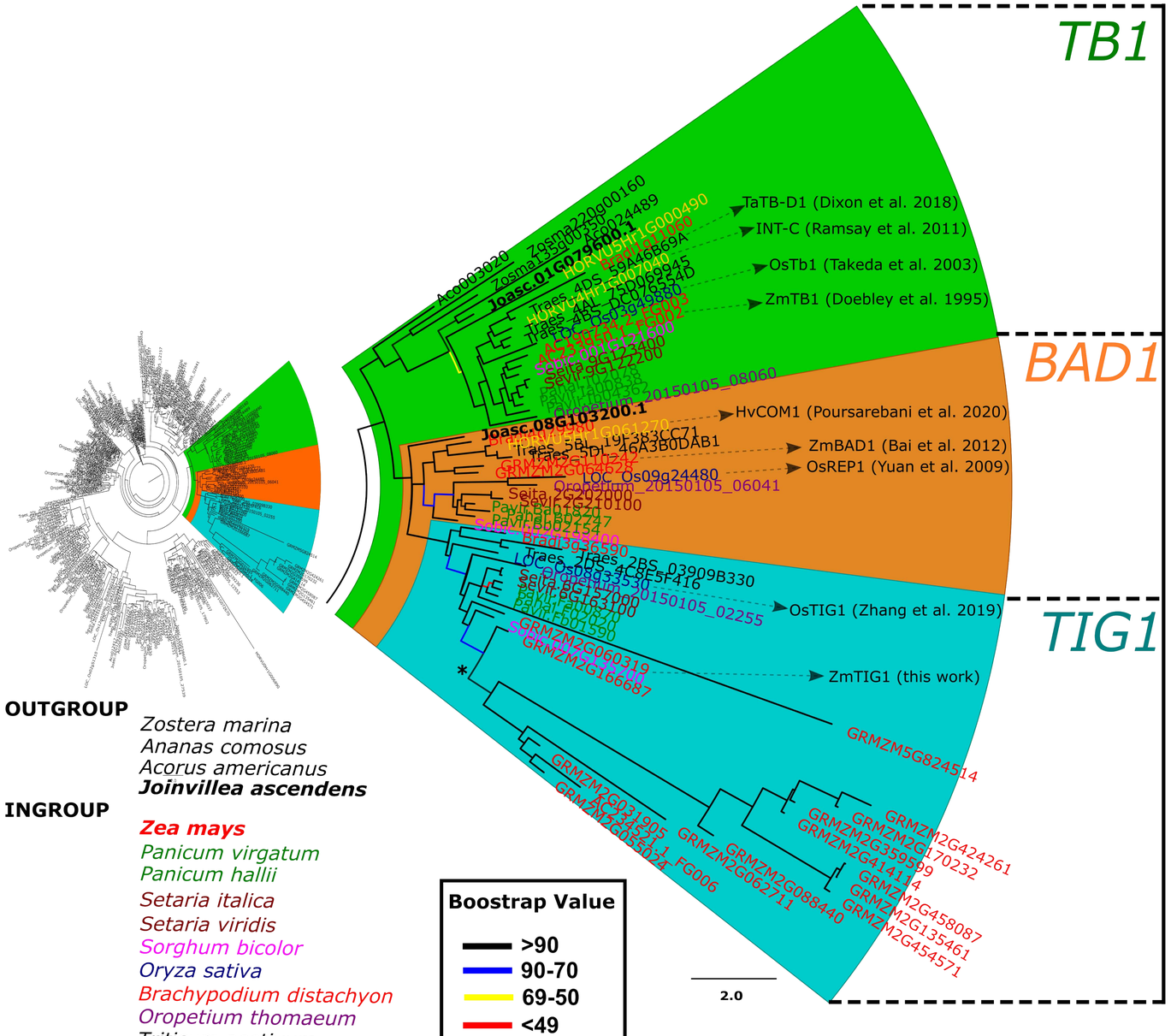

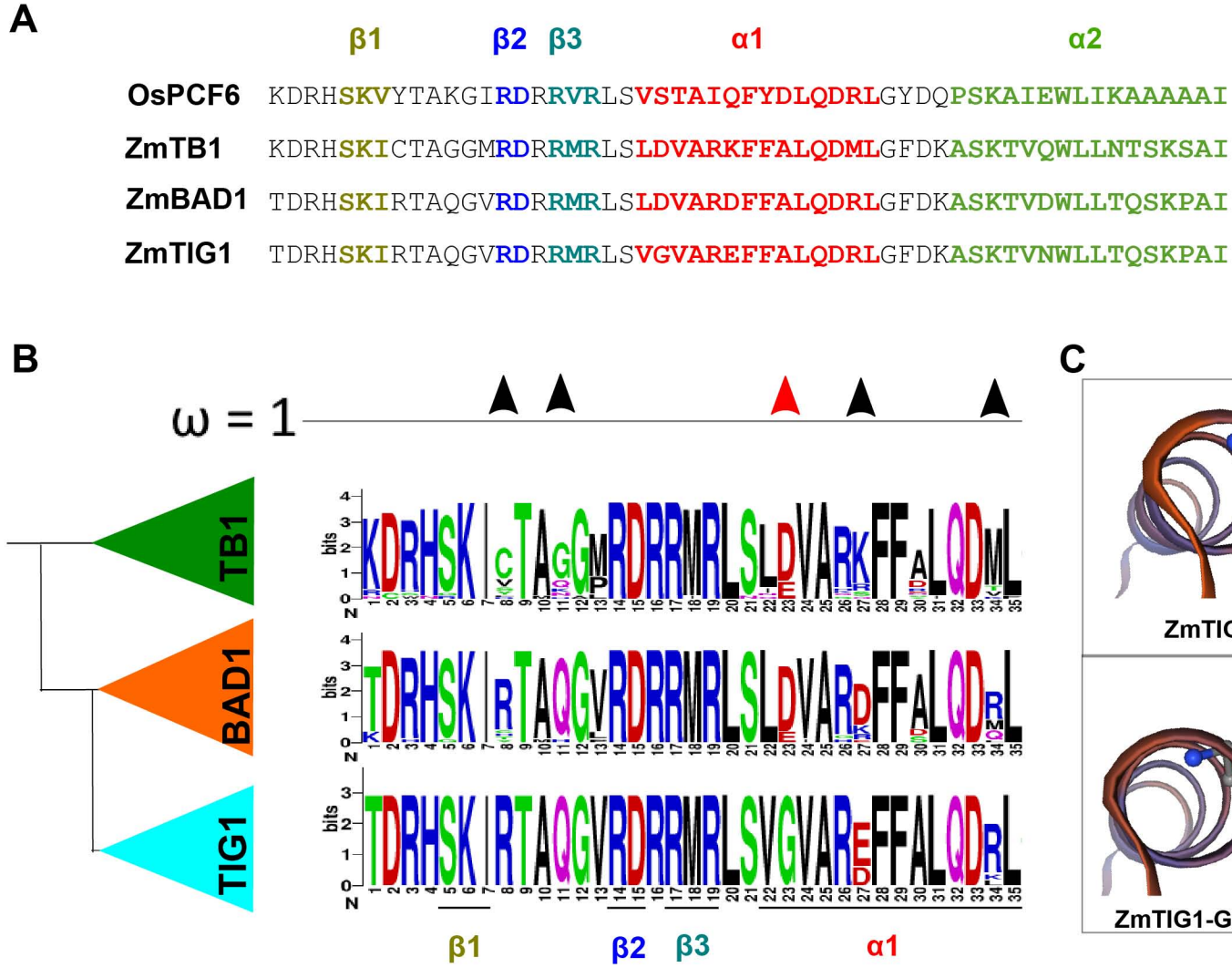

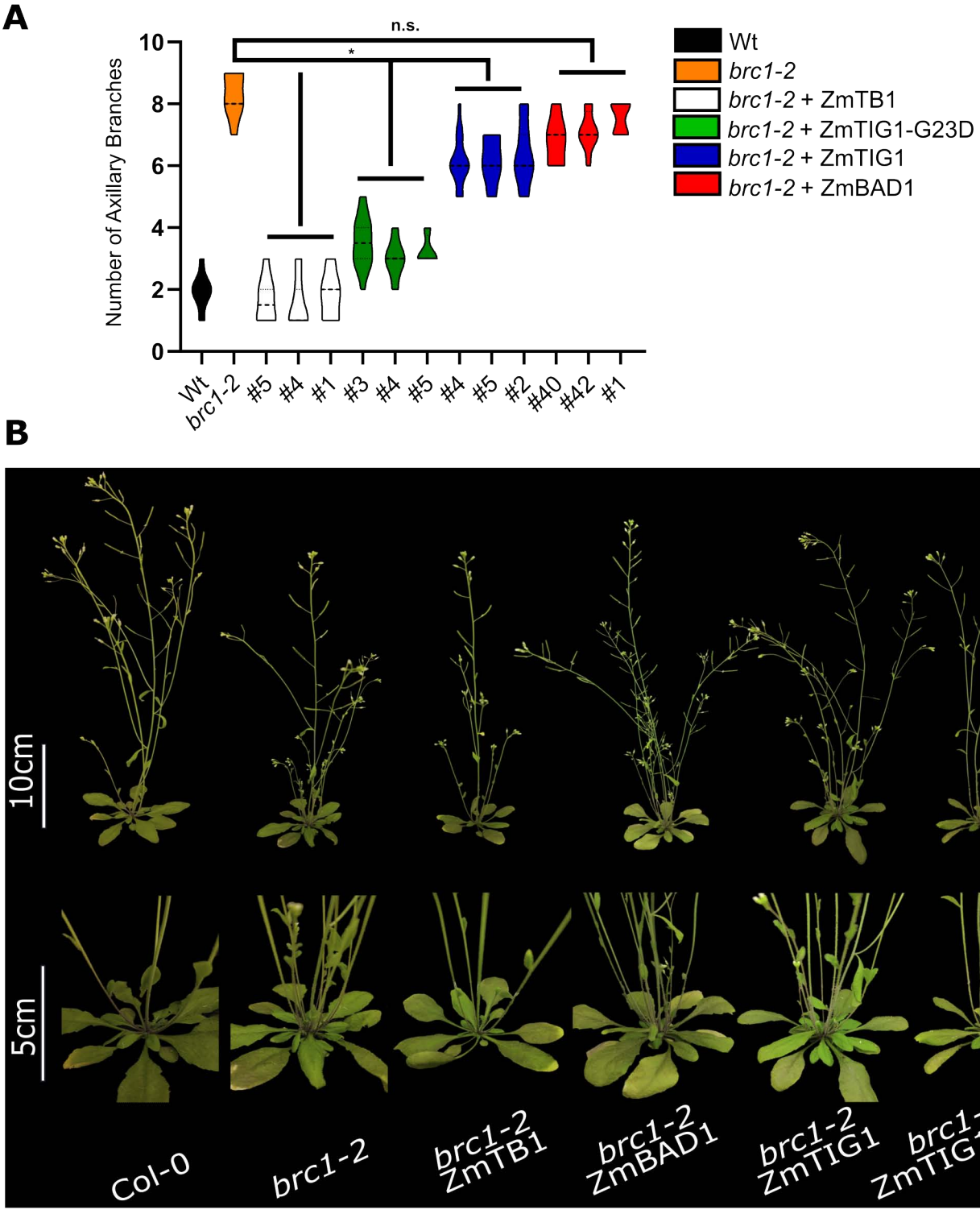

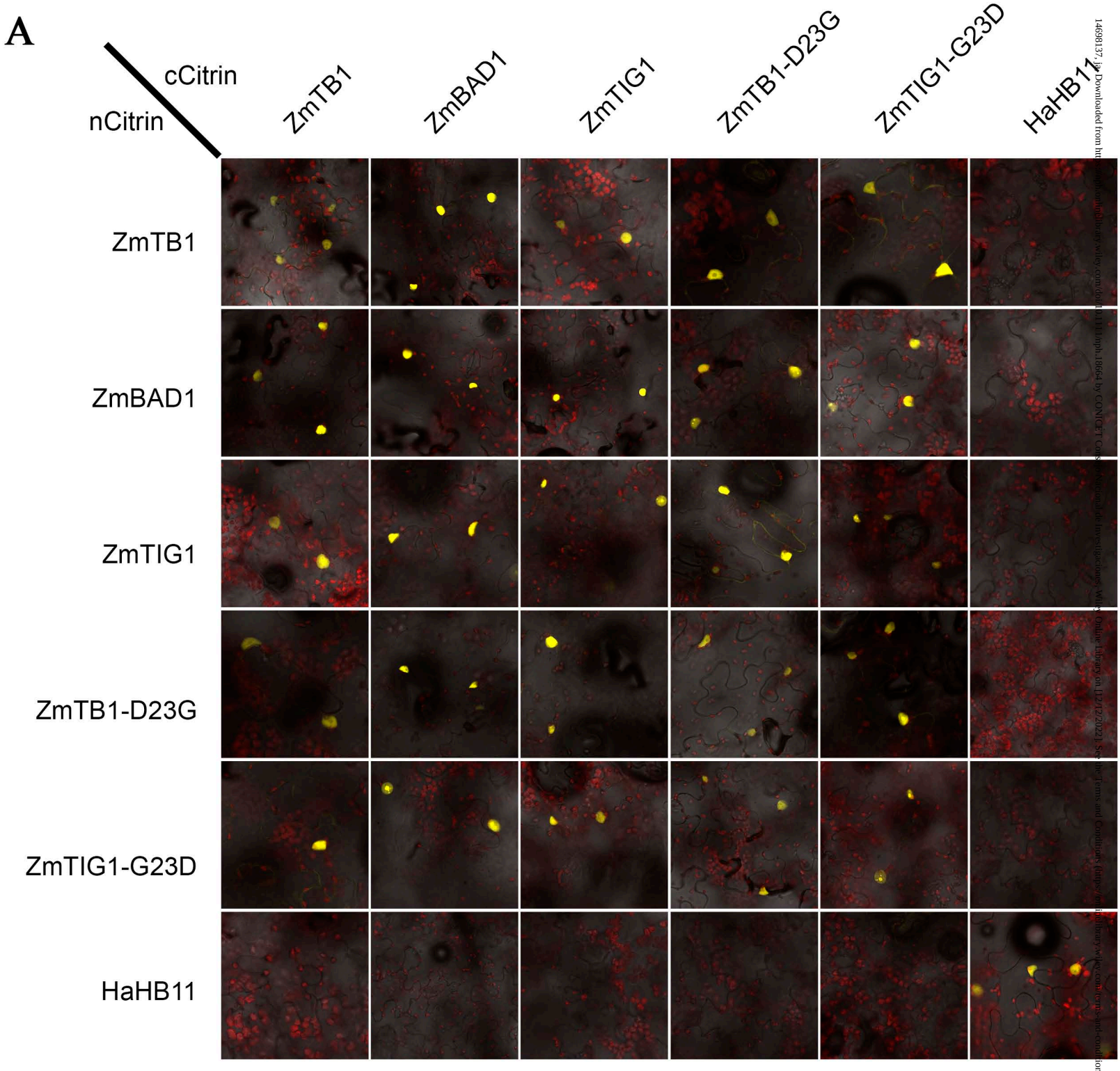

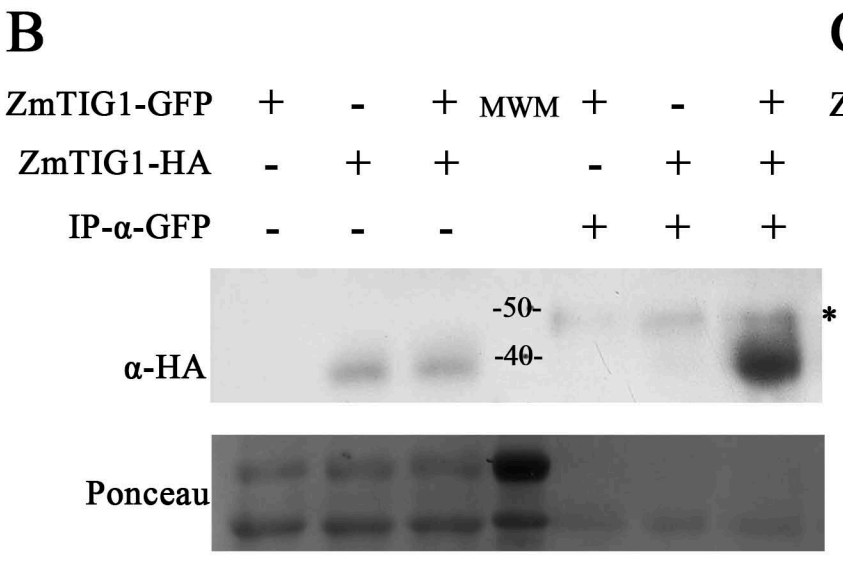

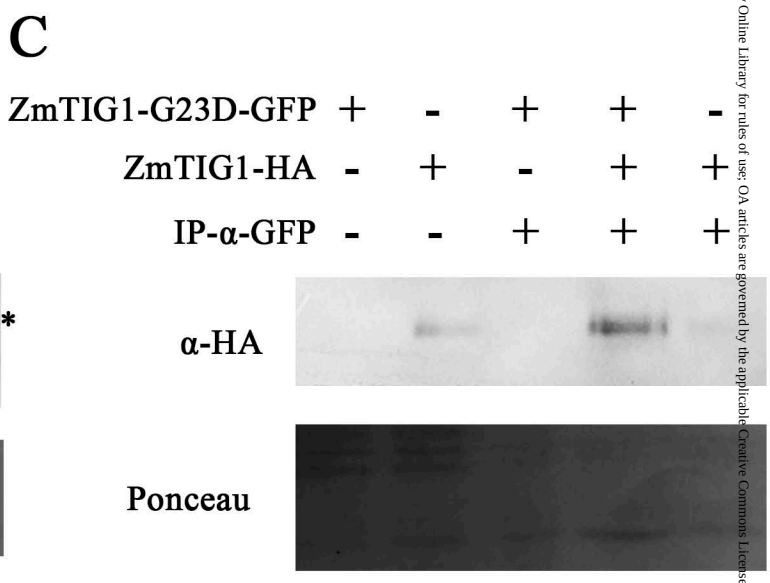

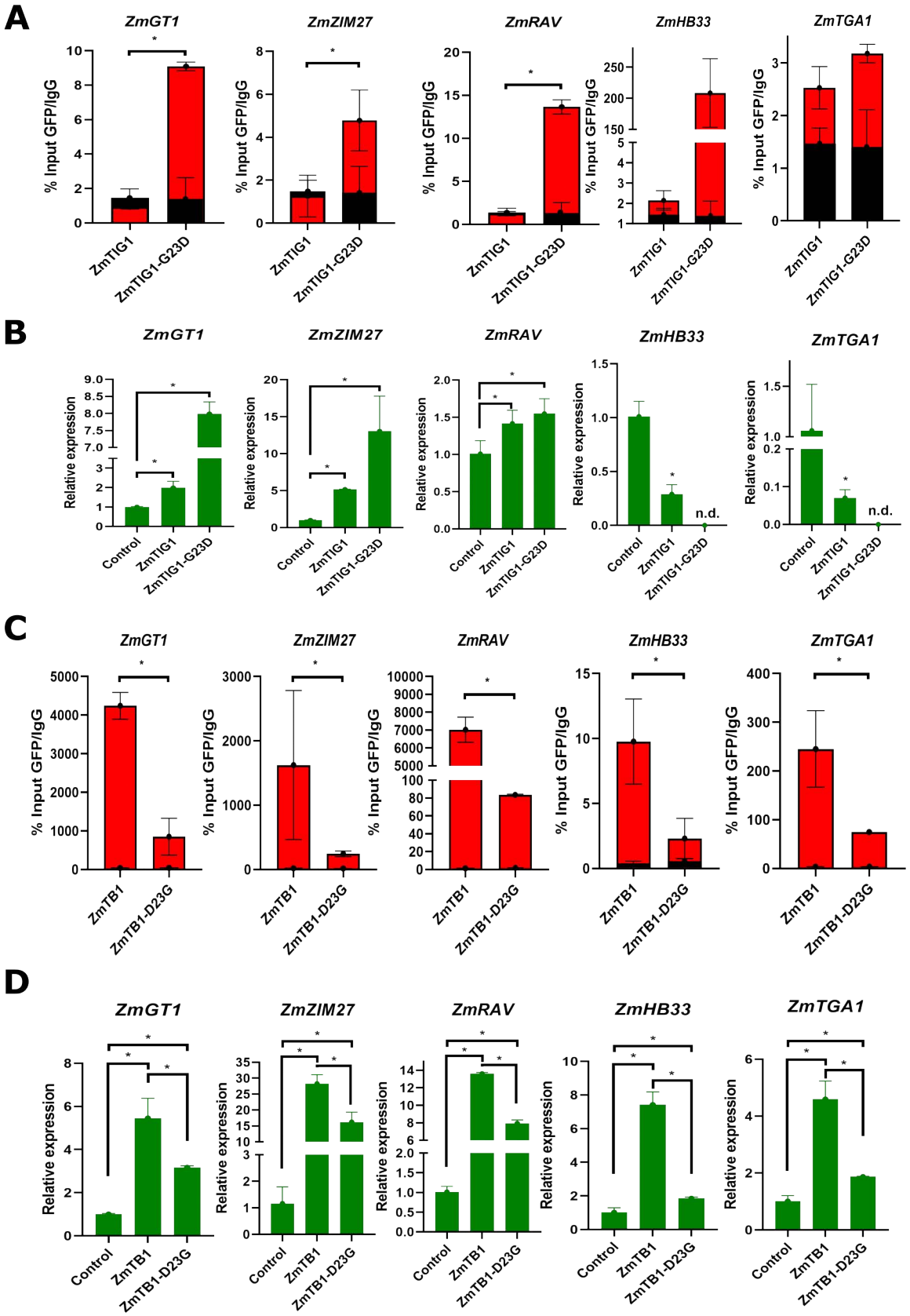

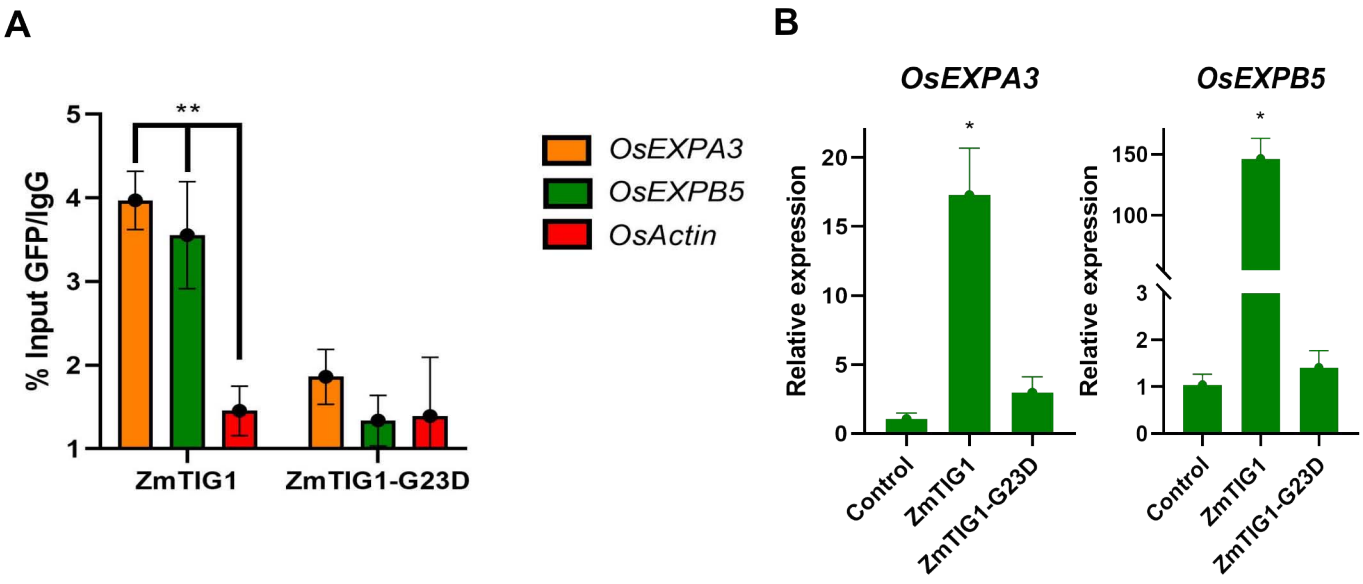

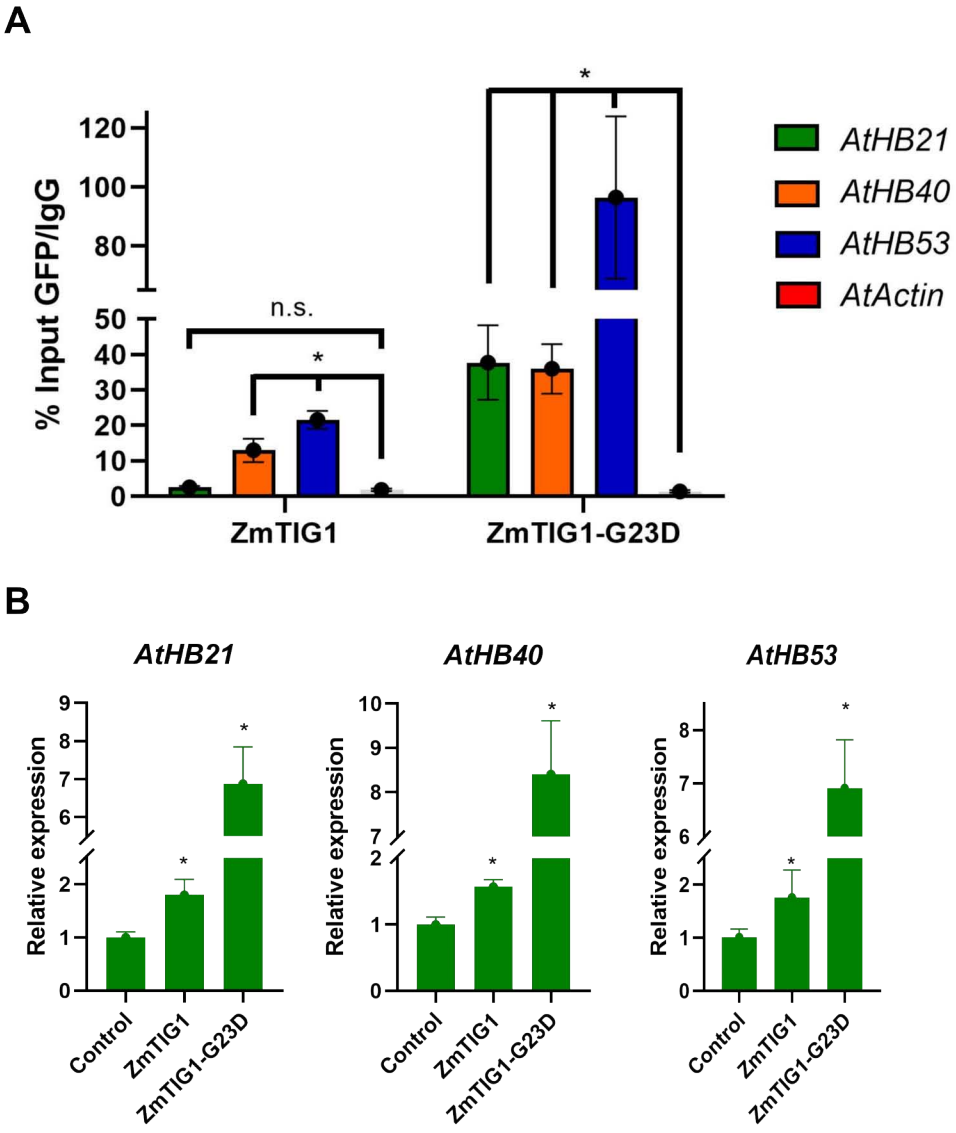

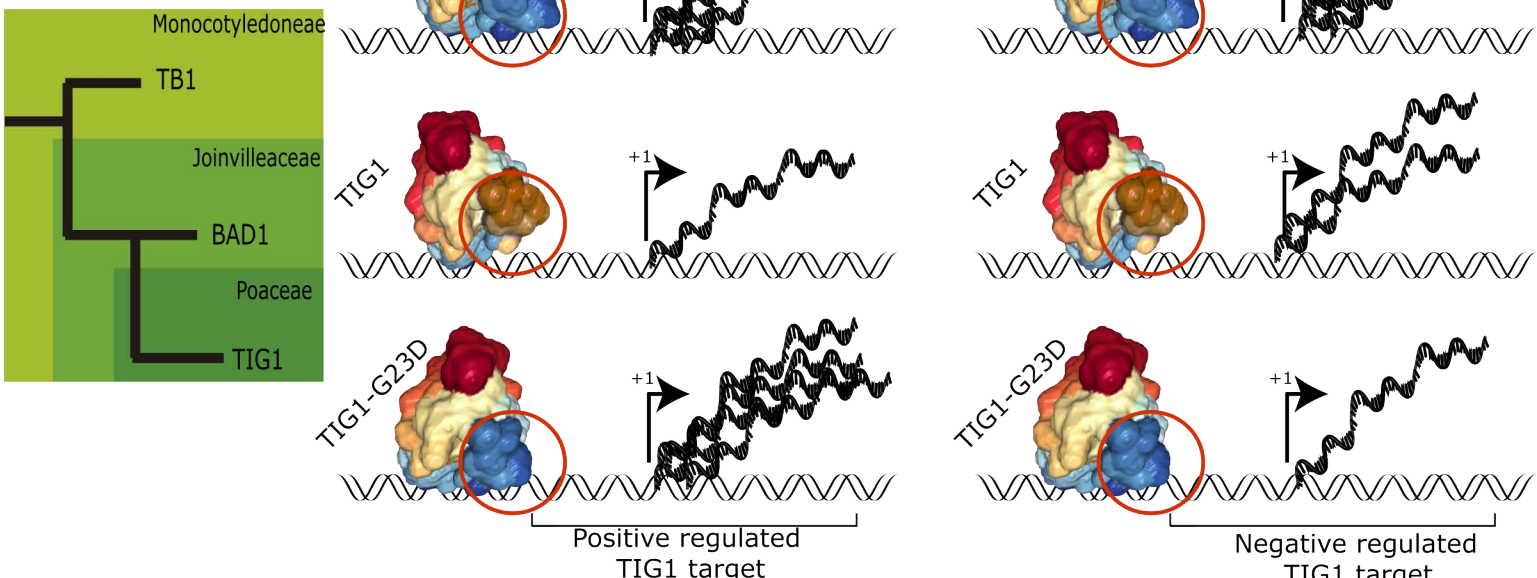
Monocotyledoneae
TB1
Joinvilleaceae
BAD1
Poaceae
TIG1
TB1
+1
TIG1
+1
TIG1-G23D
+1
Positive regulated
TIG1 target
TB1
+1
TIG1
+1
TIG1-G23D
+1
Negative regulated
TIG1 target